Influence of oxygen concentration on the kinetics of cellulose wadding degradation

Virginie Tihay, Christophe Boulnois, Philippe Gillard

Influence of oxygen concentration on the kinetics of cellulose wadding degradation

Virginie Tihay*, Christophe Boulnois, Philippe Gillard

Laboratoire PRISME, UPRES EA 4229, IUT de Bourges, 63 avenue de Lattre de Tassigny, 18020 Bourges Cedex, France
*Corresponding author. Tel.: +33 248 238 475; fax: +33 248 238 471; e-mail: vtihay@bourges.univ-orleans.fr

Abstract

The kinetics of thermal decomposition of cellulose wadding was investigated from TG-MS experiments. Different oxygen concentrations in the atmosphere and several heating rates were used to study the influence of oxygen concentration on the mass loss of the sample and on the emission of gases. A shift and an amplitude variation of the DTG curves as well as an increase of the emission of gases such as CO and CO_2 were observed. Then, a kinetic model was proposed to predict the mass loss of the cellulose wadding. Three stages were considered: the cellulose pyrolysis, the char oxidation and the decomposition of calcium carbonate. For the pyrolysis, the kinetic parameters were expressed according to the partial pressure of oxygen. For the char oxidation, a power law was used to account for the influence of oxygen whereas the other kinetic parameters were considered constant regardless of oxygen concentration. The decomposition of calcium carbonate was modelled by a first order influenced by the pressure of CO_2.

Keywords: thermal decomposition; gas product; oxygen influence.

1. Introduction

To protect the environment and reduce energy consumption, the use of recycled materials has attracted growing interest worldwide. The construction sector has thus seen increased utilisation of ecological materials such as cellulose wadding. This material is a good alternative to mineral wool and is economically very competitive. Cellulose wadding is actually made from recycled newsprint which is an abundant raw material and cheap. Its thermal and acoustic capabilities, its air permeability and moisture behaviour allow it to compete with the insulating plants such as flax, hemp and wood fibber. Given the increasing use of this material, it seems necessary to deepen the knowledge about its thermal degradation. The purpose of this study is to describe and model the influence of the oxygen concentration in atmosphere on the kinetics of thermal decomposition of cellulose wadding.
The decomposition kinetics of cellulose-based materials has been extensively investigated. However, most of them have either studied their pyrolysis [1-6] or combustion [7-8]. Few studies have examined simultaneously the thermal degradation of these materials in inert and oxidizing atmosphere. These works have highlighted the influence of oxygen on the mass loss [9], the gaseous products [9-11] and the kinetics [10-16]. However, there are still questions

about the influence of oxygen on thermal degradation of cellulosic materials and how to model the different steps.
In an attempt to provide answers to these questions, this study investigates the decomposition kinetics of cellulose wadding under different oxygen concentrations by examining the relationship between oxygen concentration, decomposition behaviour, gas emission and kinetic parameters. For this purpose, thermogravimetric analyses were carried out in order to describe the thermal decomposition of cellulose wadding. Then, the evolution of gases released during the pyrolysis and the combustion was determined by a coupling TG-MS. Finally, a kinetic study based on three stages was conducted to predict the mass loss of the sample for the different oxygen concentrations. With the kinetic parameters obtained, the influence of oxygen concentration was highlighted.

2. Material and methods

2.1. Sample

The experiments were carried out with cellulose wadding made with recycled paper and used to insulate unoccupied attic spaces and the floors. The properties of the cellulose wadding are presented in Table 1. The cellulose wadding consists mostly of cellulose together with a little fraction of hemicellulose and additives. These additives are responsible for the high mineral content. The aluminium and boron are usually added to recycled paper to improve its fire resistance and increase its resistance to insects and rodents. Other minerals are additives from the paper coating process such as pigments and calcium carbonate.

2.2. Thermogravimetric/mass spectrometric analysis

A Setsys 16/18 Setaram thermobalance coupled to a Balzers QMS 200 mass spectrometer was used to investigate the pyrolysis and the combustion of the cellulose wadding. The samples were heated from the ambient temperature to 800°C with five heating rates: 2, 5, 10, 20 and 30°C min^{-1} in an alumina crucible. The mass of the sample was equal to 5 mg to avoid the possible temperature gradient in the sample and ensure the kinetic control of the process. Argon, air or mixtures of these gases were introduced into the device in order to perform experiments under different oxygen molar percentages in the atmosphere: 0, 5.25, 10.5, 15.75 and 21%. These rates were selected to represent the compositions occurring between an inert atmosphere (0%) and air (21%). The total gas flow was equal to 20 mL min^{-1}. To characterize the TGA experiments, the following quantities were used:

- DTG corresponded to the derivative of the mass vs. time, divided by the initial mass of sample (°min^{-1}).
- T_i represents the temperature at which the i^{th} peak of DTG is maximum. The corresponding DTG value was noted DTG_i.
- X_{800} corresponds to the remaining part of the mass at 800°C (%).

During the TGA experiments, a portion of volatile products was led to the ion source of the mass spectrometer through a transfer line. The transfer line was heated and maintained at a temperature of 150°C to prevent the condensation of the volatile gases released during the thermal decomposition. The mass spectrometer was operated at 70 eV electron energy. Selected mass spectrometric intensities up to 100 were measured as functions of temperature. The ion curves close to the noise level were omitted. In this work, we focused only on the ion intensities measured for m/z=44, 40, 32, 28, 18 and 15. These values are characteristic for the

main gaseous products released during the pyrolysis and the combustion of cellulose wadding [2, 10, 17-18]: CO_2 (m/z=44), CO (m/z=28), H_2O (m/z=18) and CH_4 (m/z=15) and for the carrier gases: Ar (m/z=40) and O_2 (m/z=32). The mass spectrometric intensities were normalised by the initial sample mass and by the sum of intensities corresponding to the carrier gas (m/z=40 and/or 32) multiplied by their proportion. For each experiment, the background (corresponding to the initial gas concentration in the mass spectrometer) was also subtracted to these measurements. All experiments were carried out at least three times to ensure the reproducibility.

3. **Experimental results and Discussion**

3.1. Thermal decomposition characteristics

The mass loss of cellulose wadding is shown on Figure 1 for different oxygen concentrations at 10°C/min. The mean characteristics for all heating rates are summarized in Table 2. For these experiments, the standard deviation is less than 1% for temperature and X_{800} and 6% for DTG. Four steps of decomposition appear on the curves. The first mass loss between 50 and 100°C can be correlated with the sample dehydration. Between 308 and 342°C (depending on the heating rate), the most significant mass loss occurs. It corresponds to the depolymerization of cellulose [1, 4, 7, 10]. Increasing oxygen content from 0 to 21% shifts the maximum of this stage to lower temperatures and raises the maximum DTG (Table 2). Under an oxidizing atmosphere, a third stage takes place between 415 and 489°C. This corresponds to the char oxidation. This step is also influenced by the oxygen content. As for the cellulose depolymerization, increasing the oxygen concentration tends to shift the oxidation to lower temperatures and to raise the maximum DTG. For all atmospheres, a last step appears between 616 and 725°C because of the thermal decomposition of calcium carbonate [19-20]. For inert atmosphere, the decomposition occurs at lower temperature than for oxidizing atmospheres. However, contrary to the two previous reactions, the oxygen content does not seems influence the decomposition. The shift of the curves under oxidizing atmosphere may be due to the CO_2 present in the carrier gas (about 1.9 kPa) [20]. Although the oxygen content influences the kinetic of the degradation, at 800°C, X_{800} is almost constant (around 16.9%) when the oxygen concentration is not zero. It corresponds about to the ash content (Table 1). For experiments under argon, X_{800} is higher (around 35%). This difference is due to the char oxidation, which leads to an extra mass loss of the sample under atmosphere with oxygen.

3.2. Gas product analysis

Figure 2 shows the mass spectrometric evolution profiles of H_2O (m/z=18), CO_2 (m/z=44), CO (m/z=28) and CH_4 (m/z=15) for 30°C/min and the different oxygen concentrations. Contrary to the other gases, the H_2O formation process begins before 200°C because of the evaporation of the sample moisture. After 200°C, the amounts of H_2O, CO_2, CO and CH_4 increase significantly with a maximum peak around 340°C corresponding to the cellulose pyrolysis. A further increase in the amount of CH_4 appears after 400°C for the experiment under argon, whereas CH_4 is not detected for the experiments under oxidative atmospheres. At the same temperatures, for experiments with oxygen, a second peak (or shoulder) appears around 450°C for CO_2, CO and H_2O. These gaseous evolutions confirm that this step corresponds to the oxidation of char and of pyrolysis gases leading to the production of CO_2, CO and H_2O. Finally, above 600°C, a release of CO_2 and CO is observed. These emissions result from thermal decomposition of calcium carbonate according to the following reaction:

$$CaCO_{3(s)} \rightarrow CaO_{(s)} + CO_{2(g)} \quad (1)$$

In addition to the appearance of oxidative steps, the amount of oxygen present in the atmosphere also influences the amount of gas emitted. The emission of gaseous species increased with the concentration of oxygen. The most significant increase concerns CO and CO_2 for which the intensity is multiplied by about 100 between inert atmosphere and air. These differences between oxygen-containing atmosphere and argon are mainly caused by the oxidation reaction of char and gaseous species. The effect of ambient oxygen concentration is less important on the evolution of CH_4 and H_2O. Their intensity is indeed multiplied by 5 and 10 respectively. We note also that there is little difference between the atmospheres containing 0 and 5.25% of O_2 and 15.75 and 21% of O_2. All these results are consistent with the literature [9, 11-12, 16].

4. **Kinetic modelling: Results and Discussion**

The kinetics of heterogeneous condensed phase reactions is usually described by the following equation [21]:

$$\frac{d\alpha}{dt} = \beta \frac{d\alpha}{dT} = f(\alpha)k(T) = f(\alpha)A\exp\left(-\frac{Ea}{RT}\right) \quad (2)$$

where α is the degree of conversion, t is the time, T is the absolute temperature, β is the constant heating rate, k(T) is the Arrhenius rate constant, A and Ea are the Arrhenius parameters (pre-exponential factor and activation energy, respectively), R is the gas constant and $f(\alpha)$ is the reaction model. The reaction model may take various forms, some of which are shown in Table 3.

4.1. Identification of the kinetic scheme

The kinetic scheme of thermal degradation cellulose wadding was identified using the dependence of the activation energy Ea on the conversion α. According to Vyazovkin [22], this dependence can be considered as a source of kinetic information. The activation energy was calculated for all oxygen concentrations with the isoconversional method of Friedman [23]. This method has indeed the advantage to give unambiguous (i.e. independent of $f(\alpha)$-model) value of activation energy related to a given conversion. The isoconversional method proposed by Friedman [23] is based on using the logarithm form of Eq. (2):

$$\ln\frac{d\alpha}{dt} = \ln f(\alpha) + \ln A - \frac{Ea}{RT} = \ln A' - \frac{Ea}{RT} \quad (3)$$

where $A' = A.f(\alpha)$

The degree of conversion was calculated with:

$$\alpha = \frac{m - m_{200}}{m_{800} - m_{200}} \quad (4)$$

where m is the mass of the sample, m_{200} and m_{800} are the sample mass at 200°C and 800°C, respectively. This expression allows eliminating the drying stage, during which the moisture of the sample vaporizes.

By assuming that the reaction model $f(\alpha)$ is independent of the heating rate, $f(\alpha)$ can also be considered as constant at a given conversion. This assumption corresponds to the basic

principle of the isoconversional methods. Therefore, the activation energy was obtained using the following equation:

$$\frac{d\ln\left.\frac{d\alpha}{dt}\right|_{\alpha}}{dT^{-1}} = -\frac{Ea_{\alpha}}{R} \quad (5)$$

where $\ln\left.\frac{d\alpha}{dt}\right|_{\alpha}$ and Ea_{α} are respectively $\ln\frac{d\alpha}{dt}$ (calculated from DTG curves) and the activation energy at a given degree of conversion α.

Figure 3.a shows the activation energy in function to the degree of conversion for the different oxygen concentrations. For a conversion lower than 0.2, an increasing dependence of Ea on α is observed. This tendency is characteristic of competing reactions [22]. This phase corresponds to the start of cellulose pyrolysis. It is affected by competition among decomposition of individual macromolecules and intermolecular associates. For a conversion between 0.2 and 0.55 (for oxidizing atmosphere) or 0.75 (for inert atmosphere), the activation energy varies little. The curve has a small inflection around 0.35 or 0.5 for oxidizing and inert atmosphere respectively. This change of activation energy is due to the significant release of gas. The diffusion of gas through the surface layer of the solid becomes gradually the rate limiting step of the decomposition [22], which modifies slightly Ea. Apart from this small change, the activation energy can therefore be considered almost constant for a given oxygen concentration. The mean values are given in Table 4. These values are consistent with the depolymerisation of cellulose by transglycosylation [7]. They fall into the range usually given in the literature for pure cellulose [3-7] and paper [24-26]. The activation energy of pyrolysis of cellulose wadding decreases when the oxygen concentration increases from 0 to 21%. That highlights that at least the two competitive reactions occur under oxidative atmosphere: the depolymerisation of cellulose and an oxidative pyrolysis. The pyrolytic process of cellulose wadding is thus enhanced by heterogeneous oxidation and the oxygen promoted bond cleavage. The dependence between the mean value of Ea and the oxygen amount can be expressed as follows for the pyrolysis stage ($0.2<\alpha<0.55$):

$$Ea_1 = 207.0 - 129.1P_{O_2} \quad (r^2 = 0.99) \quad (6)$$

where P_{O_2} is the partial pressure of oxygen (in atm).

To determine the influence of oxygen concentration on the pre-exponential factor, ln A' was calculated in function to α by using Eq. 3. Figure 3.b presents the results in function to the activation energy for the pyrolysis of cellulose under argon. As with other concentrations, ln A' and the activation energy are related by a linear relationship over this interval (0.05-0.5). As the reaction model $f(\alpha)$ does not depend of Ea, we can deduce that ln A and Ea are linked by an isokinetic relationship. Thus, for the pyrolysis of cellulose wadding, the preexponential factor can be estimated by the following equation:

$$\ln A_{\alpha} = a.Ea_{\alpha} + b \quad (7)$$

Between 0.6 and 0.9, the shape of Ea vs. α changes for the oxidizing atmospheres. This coincides with the oxidation of char. Unlike the previous reaction, there is no plateau on this interval which is characteristic of multiple reactions. Between 0.6 and 0.75, there is a competition between the pyrolysis and the char oxidation. Between 0.75 and 0.9, the decomposition of calcium carbonate starts, while the char oxidation is not completely finished. As many reactions occur simultaneously between 0.6 and 0.9, it is more difficult to determine the influence of oxygen on char oxidation. However, when the pyrolysis is stopped (for a conversion of 0.8), the activation energy is almost constant whatever the concentration.

We can therefore infer that the activation energy for char oxidation does not vary with the amount of oxygen.
Between 0.9 and 1, the shape of the curve changes again. This corresponds to the decomposition reaction of calcium carbonate. As for the oxidation of char, no plateau can be shown on this interval. It is therefore not possible to determine the activation energy of the decomposition with this method.

4.2. Kinetic model for cellulose wadding under oxidizing atmosphere.

Given the previous results, the kinetic model must be decomposed into three stages corresponding to the pyrolysis of cellulose, the char oxidation and the decomposition of calcium carbonate:

$$\text{Cellulose wadding} \xrightarrow{1} \upsilon_1 \text{Volatiles}_1 + \upsilon_2 \text{Char} + (1-\upsilon_1-\upsilon_2)\,\text{Calcium carbonate}$$

$$\upsilon_2 \text{Char} \xrightarrow{2} \upsilon_3 \text{Volatiles}_2 + (\upsilon_2-\upsilon_3)\,\text{Ash}$$

$$(1-\upsilon_1-\upsilon_2)\text{Calcium carbonate} \xrightarrow{3} \upsilon_4 \text{Volatiles}_3 + (1-\upsilon_1-\upsilon_2-\upsilon_4)\,\text{Ash}$$

where υ_i is the yield coefficient of the volatiles, tar or char.

The degree of conversion α_i for the i^{th} reaction corresponds to:

$$\alpha_i = \frac{m_i - m_{i,0}}{m_{i,f} - m_{i,0}} \quad (8)$$

where m_i is the mass of solid decomposing during the i^{th} reaction. The subscripts 0 and f refer to the initial and residual amounts, respectively.

The rate expression for the pyrolysis of cellulose is given by:

$$\frac{d\alpha_1}{dt} = A_1.f(\alpha_1).\exp\left(-\frac{Ea_1}{RT}\right) \quad (9)$$

where $f(\alpha_1)$ represents one of the reaction models of Table 3.
The dependency of Ea_1 with the oxygen concentration is taken into account with Eq. 6. According to Eq. 7, the preexponential factor is linked with Ea_1 by:

$$\ln A_1 = a.Ea_1 + b \quad (10)$$

The kinetic equation for the char oxidation is:

$$\frac{d\alpha_2}{dt} = A_2.(\alpha_1-\alpha_2)^{n_2}.P_{O_2}^{m_2}.\exp\left(-\frac{Ea_2}{RT}\right) \quad (11)$$

This expression allows highlighting that:

- Pyrolysis of cellulose and oxidation of char are competitive reactions.
- The oxidation of char takes place only in an oxidizing atmosphere.

The decomposition of calcium carbonate is represented by a first order reaction influenced by the pressure of CO_2 [20]:

$$\frac{d\alpha_3}{dt} = A_3.(1-\alpha_3).\left(1-\frac{P_{CO_2}}{P_{CO_2}^*}\right).\exp\left(-\frac{Ea_3}{RT}\right) \quad (12)$$

where $P_{CO_2}^*$ is the equilibrium pressure of CO_2 equal to 2.86 kPa. In our study, P_{CO_2} is equal to 0 for inert atmosphere and 1.9 for others.

The total conversion rate and the degree of conversion are calculated as:

$$\alpha = f_1.\alpha_1 + f_2.\alpha_2 + f_3.\alpha_3 \quad (13)$$

and

$$\frac{d\alpha}{dt} = f_1 \frac{d\alpha_1}{dt} + f_2 \frac{d\alpha_2}{dt} + f_3 \frac{d\alpha_3}{dt} \quad (14)$$

where f_1, f_2 and f_3 represent the contribution of each reaction to the global decomposition:

$$f_1 = \frac{\upsilon_1}{\upsilon_1 + \upsilon_3 + \upsilon_4} \quad (15)$$

$$f_2 = \frac{\upsilon_3}{\upsilon_1 + \upsilon_3 + \upsilon_4} \quad (16)$$

$$f_3 = \frac{\upsilon_4}{\upsilon_1 + \upsilon_3 + \upsilon_4} \quad (18)$$

Thus:

$$f_1 + f_2 + f_3 = 1 \quad (19)$$

To differentiate the contributions in an inert atmosphere, we have added an apostrophe. Therefore $f_2' = 0$.

To determine the most suitable reaction model $f(\alpha_1)$ for modelling the pyrolysis of cellulose (Eq. 9) and obtain the set of parameters for the thermal degradation of the cellulose wadding, each model presented in Table 3 were tested and the corresponding kinetic parameters were calculated. For this, the degree of conversion (α^{obs}) obtained with the experiments were compared to the calculated points (α^{cal}). The calculated values were obtained by integration of the differential system with an explicit second-order Runge Kutta method. The optimization of the kinetic parameters was performed with the gradient descent method. For each reaction model, the kinetic parameters correspond to the values for which the sum

$$S = \sum_{i=1}^{N} \left(\alpha_i^{obs} - \alpha_i^{cal} \right)^2 \quad (17)$$

is minimal. Here N is the number of point of the experimental curves.
The resulting fit can be expressed for each evaluated curve as:

$$\text{Fit}(\%) = 100 \frac{\sqrt{S}}{N} \quad (18)$$

Table 5 presents the kinetic parameters and the mean fit values for the reaction models, which best describe the experiments. Only five models of Table 3: F_1 (first-order model), F_n (n-order kinetic model), A_n (Avrami-Erofe'ev model), B_1 (Prout-Tomkins model) and D_5 (Zhuravlev, Lesokin, Tempelman model) describe the first degradation of cellulose wadding satisfactorily (Eq. 8) . The best adequacies are obtained with the n-order kinetic (F_n) model (Fig. 4) and the Prout-Tomkins (B_1) model (Fig. 5). This results are in agreement with literature [5, 25, 27]. The experimental data and the simulations are very close whatever the heating rate or the oxygen concentration. Only a few variations appear at the maximum conversion rate. The kinetic model tends to slightly underestimate its value. The oxidation of char is correctly described as well as the decomposition of calcium carbonate. The simulations under argon have a fit value slightly higher than under the oxidizing atmospheres. For the inert atmosphere, the oxidation of char was completely neglected. However, the argon used for these experiments contains a little oxygen (less than 2 ppm) what is sufficient to cause an oxidation. The simulated curves do not take into account this phenomenon that is why there is

a difference between simulations and experiments. Despite these very small differences, the kinetic approach including either the n-order model (F_n) or the Prout-Tomkins model (B_1) for cellulose degradation produces very satisfactory results.

In view of Table 5, some interesting aspects can be emphasized concerning the degradation of cellulose wadding.
The value of n calculated with the n-order or the Prout-Tomkins models are higher than those currently obtained for pure cellulose (around 1 [4-6]) but are close to that found for cellulosic paper [24, 26]. As Ea, ln A decreases when the oxygen concentration increases from 0 to 21 %. This result is consistent with the observations on the position of first DTG maximum (Fig. 1). The optimisation of the fraction f_1 clearly illustrates that the major part of the cellulose wadding is lost during the depolymerisation of cellulose.
The activation energy for the oxidation of char is around 178 kJ/mol. This value is close to those found in the literature for cellulosic paper. Kashiwagi and Nambu [24] proposed an activation energy equal to 160 kJ/mol for cellulosic paper. Wu et al. studied different types of paper and found activation energies between 101 and 182 kJ/mol [26]. The optimised reaction order for char oxidation n_2 is equal to 2.1. This value is higher than that proposed by [24] (1.8). The dependence of the char oxidation with the partial pressure seems to be well modeled with a power law. The optimised exponent n_3 is around 1.4, which is also higher than the values of literature (values between 0.5 and 1 [8,16,24]).
For the decomposition of calcium carbonate, we found an activation energy of about 193 kJ/mol. This value is consistent with the literature [19-20]. Moreover, taking into account the pressure of CO_2 can correctly model the differences in decomposition between the various atmospheres.

5. Conclusions

The influence of the oxygen concentration on the kinetics of cellulose wadding degradation was studied. The following results were pointed out:

- The oxygen in the atmosphere influences the position and amplitude of the DTG curve. Increasing the oxygen concentration tends to shift the pyrolysis and the char oxidation to lower temperatures and to raise the maximum DTG.
- The formation rate of main gases (H_2O, CO_2, CO, CH_4 and H_2) varies with temperature and is strongly correlated with the decomposition steps.
- The presence of oxygen in atmosphere increases the emission of main gaseous species. This is particularly evident for CO and CO_2, which are combustion products generated by the oxidation of char.
- The oxygen content in the atmosphere influences strongly the kinetic parameters. For the decomposition of cellulose, the activation energy decreases when the oxygen concentration increases from 0 to 21%. For the char oxidation, the activation energy can be considered as a constant whatever the oxygen content.
- A kinetic model based on three steps (pyrolysis, char oxidation and decomposition of calcium carbonate) was used to model the thermal degradation of cellulose wadding. The thermal decomposition of cellulose can be described with acceptable accuracy by a n-order model or by a Prout-Tomkins model. The char oxidation was correctly modelled by a power law including the partial pressure of oxygen.

Acknowledgment

The authors express their gratitude to Laurent Arcese for his help on numerical optimization methods.

References

[1] A. Broido, Kinetics of Solid-Phase Cellulose Pyrolysis, in F. Shafizadeh, K.V. Sarkanen, D.A. Tillman (Eds.), Thermal Uses and Properties of Carbohydraes and Lignins, Academic Press, New York, 1976, pp 19−35.
[2] P.C. Lewellen, W.A. Peters, J.B. Howard, Cellulose pyrolysis kinetics and char formation mechanism, Symp. (Int.) Combust. 16 (1977) 1471-1480.
[3] G. Varhegyi, E. Jakab, Is the Broido-Shafizadeh Model for Cellulose Pyrolysis True??, Energy Fuels 8 (1994) 1345-1352.
[4] M.J. Antal, G. Várhegyi, Cellulose Pyrolysis Kinetics: The Current State of Knowledge. Ind. Eng. Chem. Res. 34 (1995) 703−717.
[5] J. A. Conesa, J.A. Caballero, A. Marcilla, R. Font, Analysis of different kinetic models in the dynamic pyrolysis of cellulose, Thermochim. Acta 254 (1995) 175-192.
[6] J.J.M. Orfão, F.J.A. Antunes, J.L. Figueiredo Pyrolysis kinetics of lignocellulosic materials—three independent reactions model, Fuel 78 (1999) 349-358.
[7] V. Mamleev, S. Bourbigot, J. Yvon, Kinetic analysis of the thermal decomposition of cellulose: The main step of mass loss, J. Anal. Appl. Pyrolysis 80 (2007) 151 – 165.
[8] R. Bilbao, J.F. Mastral, M.E. Aldea, J. Ceamanos, Kinetic study for the thermal decomposition of cellulose and pine sawdust in an air atmosphere, J. Anal. Appl. Pyrolysis 39 (1997) 53-64.
[9] T. Kashiwagi, T.J. Ohlemiller, K. Werner, Effects of external radiant flux and ambient oxygen concentration on nonflaming gasification rates and evolved products of white pine, Combust. and Flame 69 (1987) 331-345.
[10] F. Shafizadeh, Pyrolysis and combustion of cellulosic materials, in Advances in carbohydrate chemistry Volume 22, Academic press Inc., London, 1969, pp. 419-474.
[11] D. Fairbridge, R.A. Ross, S.P. Sood, A kinetic and surface study of the thermal decomposition of cellulose powder and inert and oxidizing atmosphere, J. Appl. Polym. Sci., 22 (1978) 497-510.
[12] M.X. Fang, D.K. Shen, Y.X. Li, C.J. Yu, Z.Y. Luo, K.F. Cen, Kinetic study on pyrolysis and combustion of wood under different oxygen concentrations by using TG-FTIR analysis, J. Anal. Appl. Pyrolysis 77 (2006) 22-27.
[13] C. Vovelle, H. Mellottée, R. Delbourgo, Kinetics of the thermal degradation of cellulose and wood in inert and oxidative atmospheres, Symp. (Int.) Combust. 19 (1982) 797-805.
[14] R. Bilbao, J. F. Mastral, M. E. Aldea, J. Ceamanos, The influence of the percentage of oxygen in the atmosphere on the thermal decomposition of lignocellulosic materials, J. Anal. Appl. Pyrolysis 42 (1997) 189-202.
[15] J. Moltó, R. Font, J.A. Conesa, I. Martín-Gullón, Thermogravimetric analysis during the decomposition of cotton fabrics in an inert and air environment, J. Anal. Appl. Pyrolysis 76 (2006) 124-131.
[16] R. Font, J.A. Conesa, J. Moltó, M. Muñoz Kinetics of pyrolysis and combustion of pine needles and cones, J. Anal. Appl. Pyrolysis 85 (2009) 276-286.
[17] D.K. Shen, S. Gu, The mechanism for thermal decomposition of cellulose and its main products, Bioresour. Technol. 100 (2009) 6496-6504.
[18] R. Alen, E. Kuoppala, P. Oesch, Formation of the main degradation compound groups from wood and its components during pyrolysis, J. Anal. Appl. Pyrolysis 36 (1996) 137-148.

[19] J. P. Sanders, P. K. Gallagher, Kinetic analyses using simultaneous TG/DSC measurements: Part I: decomposition of calcium carbonate in argon, Thermochim. Acta 388 (2002) 115-128.
[20] J. M. Criado, M. González, J. Málek, A. Ortega, The effect of the CO_2 pressure on the thermal decomposition kinetics of calcium carbonate, Thermochim. Acta 254 (1995) 121-127.
[21] S. Vyazovkin, Modification of the integral isoconversional method to account for variation in the activation energy, J. Comput. Chem. 22 (2001) 178-183.
[22] S. Vyazovkin, A Unified Approach to Kinetic Processing of Nonisothermal Data, Int. J. Chem. Kinet. 28 (1996) 95-101.
[23] H.L. Friedman, Kinetics of Thermal Degradation of Char-Forming Plastics from Thermogravimetry. Application to a Phenolic Plastic, J. Polym. Sci. Pol. Sym., 6 (1964) 183-195.
[24] T. Kashiwagi, H. Nambu, Global kinetic constants for thermal oxidative degradation of a cellulosic paper, Combust. and Flame 88 (1992) 345-368.
[25] J.G. Reynolds, A.K. Burnham, Pyrolysis Decomposition Kinetics of Cellulose-Based Materials by Constant Heating Rate Micropyrolysis, Energ. Fuel, 11 (1997) 88-97.
[26] C.H. Wu, C.-Y. Chang, J.P. Lin, J.Y Hwang, Thermal treatment of coated printing and writing paper in MSW: pyrolysis kinetics, Fuel 76 (1997) 1151-1157.
[27] R. Capart, L. Khezami, A. K. Burnham, Assessment of various kinetic models for the pyrolysis of a migrogranular cellulose, Thermochim. Acta, 417 (2004) 79-89.

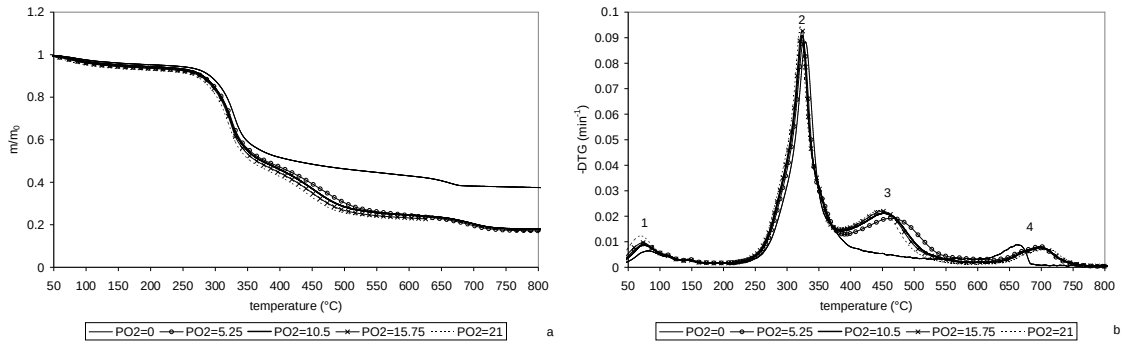

Fig. 1. Mass loss of the cellulose wadding for different oxygen concentrations at 10°C/min.

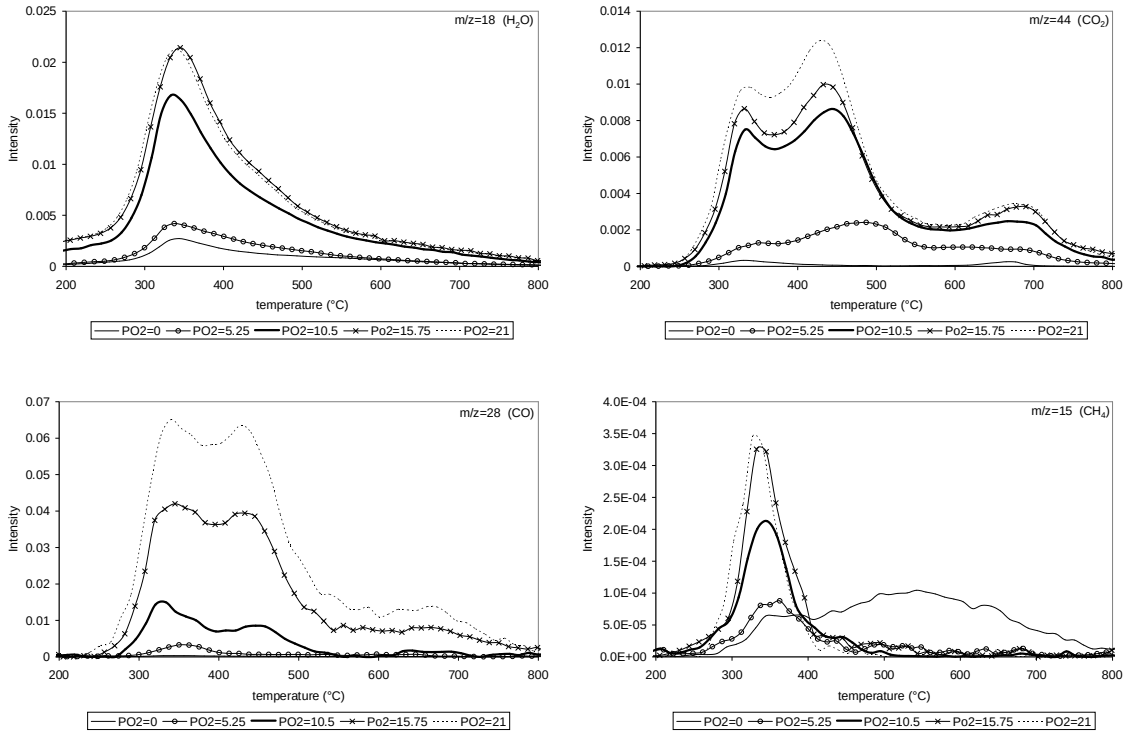

Fig. 2. Ion intensities measured for m/z=18 (H_2O), m/z=44 (CO_2), m/z=28 (CO) and m/z=15 (CH_4) for different oxygen concentrations at 30°C/min.

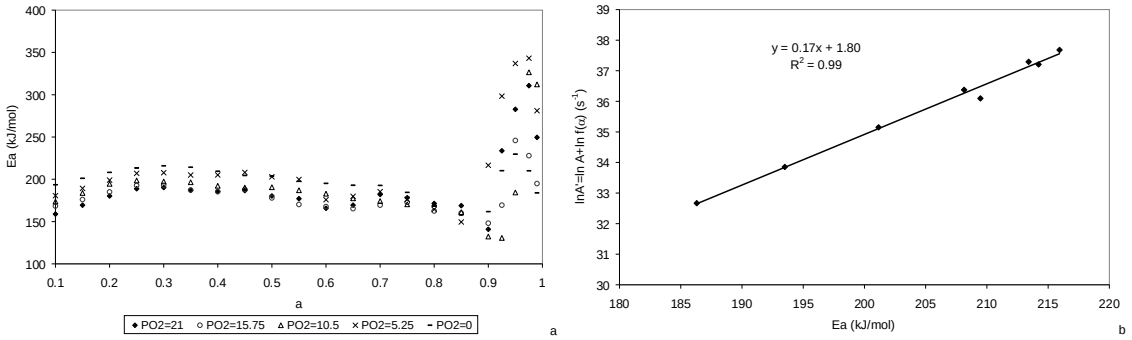

Fig. 3. a) Dependency of Ea on α. b) ln A' in function to Ea for the degradation under argon.

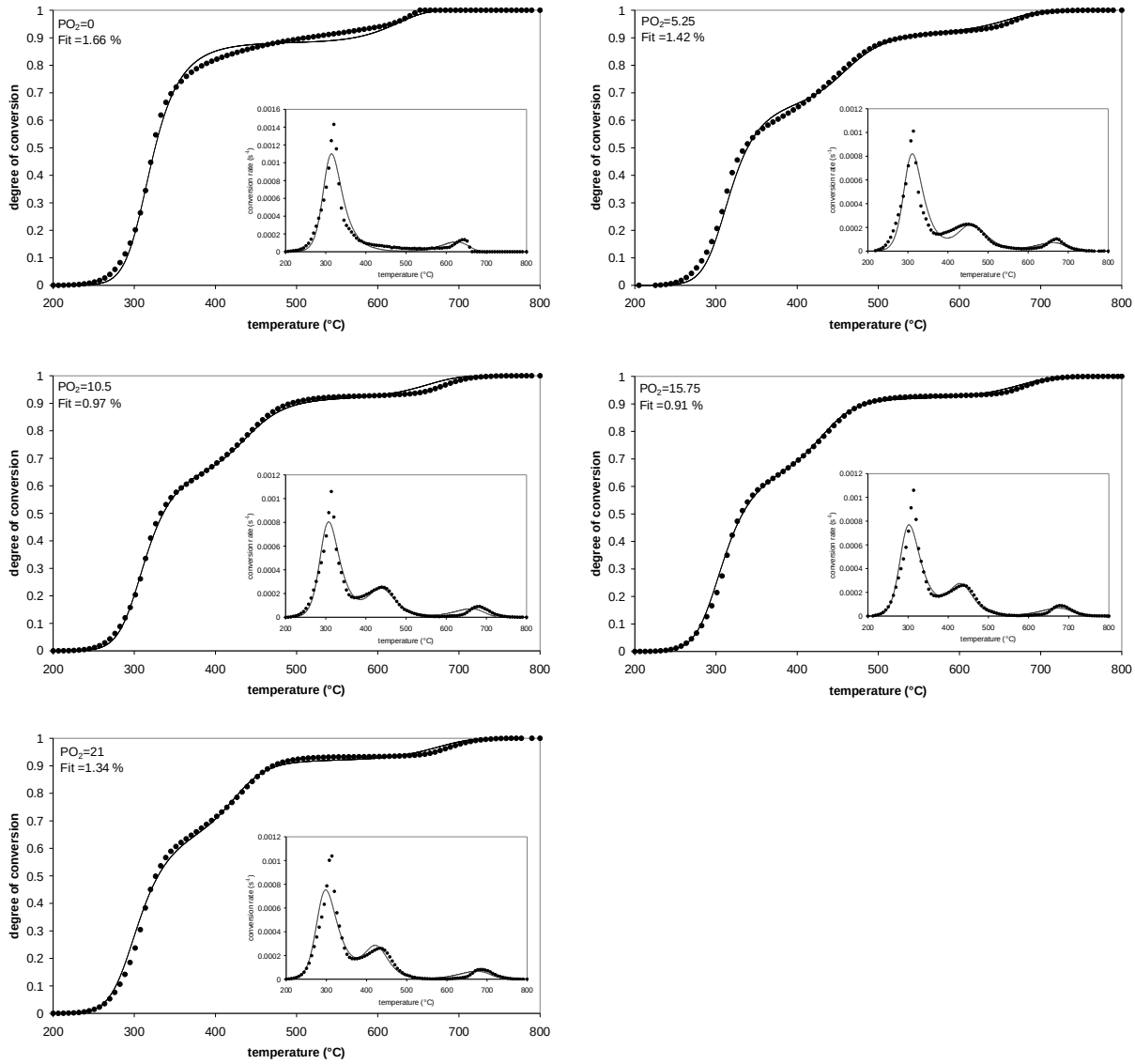

Fig. 4. Experimental data (●) and values calculated with the n-order model (line) for different oxygen concentrations at 5°C/min.

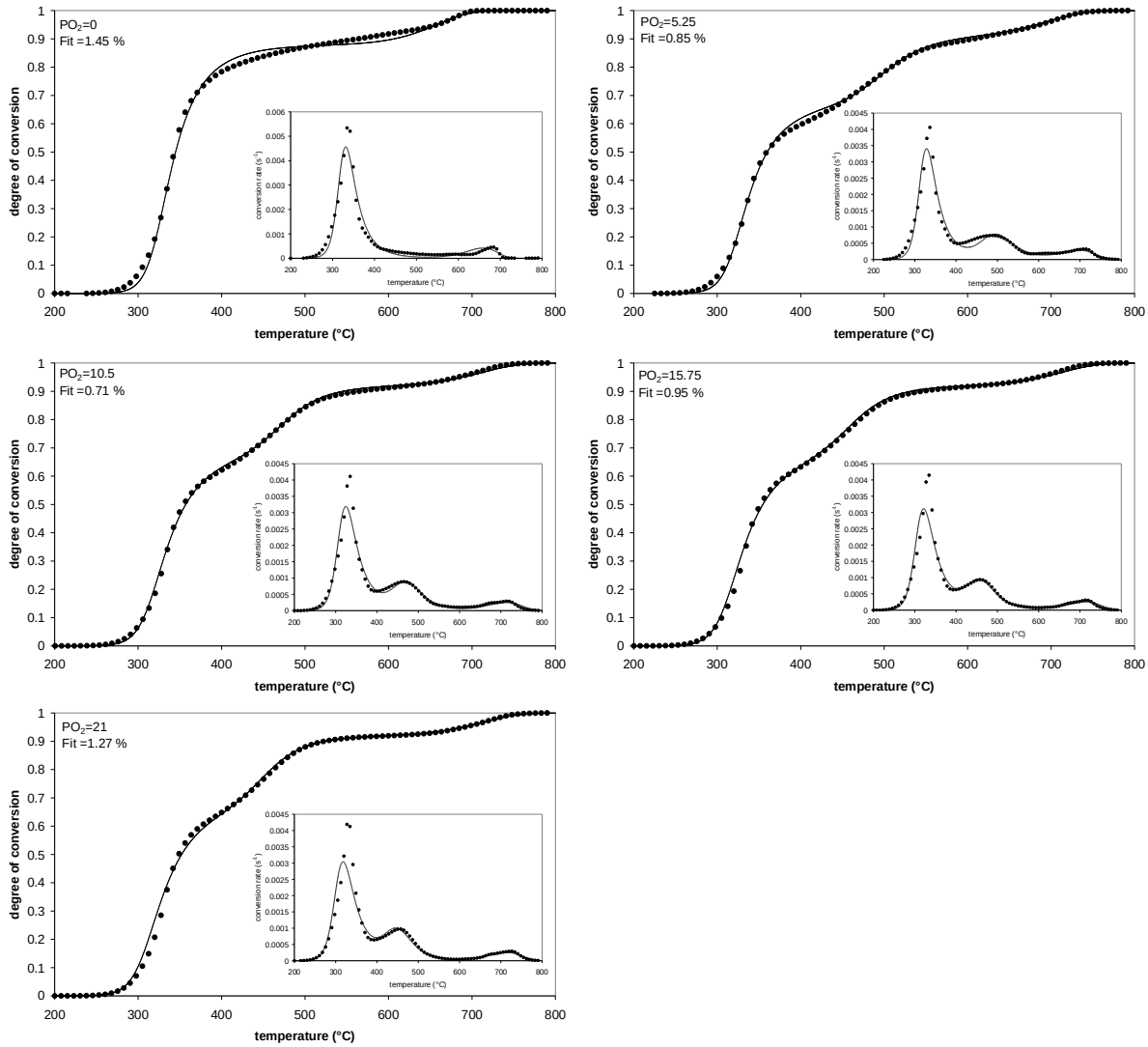

Fig. 5. Experimental data (●) and values calculated with the Prout-Tomkins model (line) for different oxygen concentrations at 20°C/min.

Table 1.
Properties of cellulose wadding

Ultimate analysis (wt %)	
C	36.37
H	5.08
O	41.85
N	<0.1
Si	7.82
Ca	5.01
Al	1.09
Mg	0.47
Fe	0.29
B	1.41
Other minerals	1.7
Heating values (MJ kg^{-1})	
Higher	12.11
Lower	10.97
Proximate analysis (wt %)	
Moisture	7.2
Ash	16.7
Combustibles	76.1

Table 2.
Degradation characteristics

Heating rate (°C/min)	Oxygen concentration (%)				
	0	5.25	10.5	15.75	21
T_1 (°C) [-DTG_1 (min^{-1})]					
2	48 [0.003]	46 [0.003]	42 [0.003]	45 [0.003]	42 [0.003]
5	61 [0.005]	60 [0.004]	64 [0.005]	57 [0.006]	58 [0.006]
10	82 [0.007]	76 [0.009]	75 [0.008]	73 [0.010]	70 [0.012]
20	93 [0.015]	91 [0.015]	89 [0.016]	88 [0.015]	85 [0.021]
30	102 [0.017]	101 [0.017]	101 [0.019]	98 [0.019]	96 [0.024]
T_2 (°C) [-DTG_2 (min^{-1})]					
2	308 [0.017]	304 [0.017]	301 [0.018]	299 [0.018]	297 [0.019]
5	320 [0.044]	317 [0.041]	314 [0.044]	313 [0.045]	311 [0.045]
10	329 [0.088]	325 [0.088]	324 [0.091]	323 [0.093]	321 [0.095]
20	338 [0.170]	335 [0.178]	333 [0.179]	332 [0.181]	331 [0.182]
30	342 [0.239]	338 [0.256]	337 [0.257]	337 [0.258]	336 [0.258]
T_3 (°C) [-DTG_3 (min^{-1})]					
2	-	437 [0.004]	424 [0.005]	419 [0.005]	415 [0.005]
5	-	454 [0.009]	438 [0.011]	438 [0.011]	432 [0.011]
10	-	463 [0.019]	451 [0.021]	449 [0.022]	446 [0.022]
20	-	487 [0.033]	464 [0.040]	458 [0.040]	454 [0.042]
30	-	489 [0.049]	465 [0.059]	463 [0.058]	456 [0.060]
T_4 (°C) [-DTG_4 (min^{-1})]					
2	616 [0.002]	663 [0.002]	666 [0.002]	665 [0.002]	670 [0.002]
5	642 [0.005]	676 [0.004]	684 [0.004]	675 [0.004]	686 [0.004]
10	662 [0.009]	699 [0.008]	698 [0.007]	698 [0.007]	712 [0.007]
20	686 [0.017]	712 [0.015]	715 [0.013]	721 [0.018]	725 [0.013]
30	685 [0.021]	718 [0.022]	722 [0.019]	717 [0.020]	725 [0.019]
X_{800} (%)					
2	35.1	17.1	16.7	17.3	16.7
5	35.0	17.2	16.7	16.9	16.7
10	35.0	17.0	17.3	16.7	16.7
20	34.2	17.0	17.0	16.9	16.8
30	35.2	16.9	16.7	17.2	16.8

Table 3.
Different models for solid decomposition

Function name		f(α)
1. Based on "order reaction"		
F_n	n-order	$(1-\alpha)^n$
2. Acceleratory α-t curves		
P_1	Power law	$n\alpha^{1-1/n}$
E_1	Exponential law	α
3. Sigmoid α-t curves		
A_n	Avrami-Erofe'ev	$n(1-\alpha)[-\ln(1-\alpha)]^{1-1/n}$
B_1	Prout-Tompkins	$\alpha^m(1-\alpha)^n$
4. Deceleratory α-t curves based on diffusion mechanisms		
R_n	Based on geometrical models	$n(1-\alpha)^{1-1/n}$
D_1	One dimensional	$\frac{1}{2}\alpha$
D_2	Two dimensional	$[-\ln(1-\alpha)]^{-1}$
D_3	Three dimensional	$\frac{3}{2}(1-\alpha)^{2/3}\left[1-(1-\alpha)^{1/3}\right]^{-1}$
D_4	Ginstling-Brounshtein	$\frac{3}{2}\left[(1-\alpha)^{-1/3}-1\right]^{-1}$
D_5	Zhuravlev, Lesokin, Tempelman	$\frac{3}{2}(1-\alpha)^{4/3}\left[(1-\alpha)^{-1/3}-1\right]^{-1}$

Table 4.
Mean activation energy for the pyrolysis of cellulose wadding

Oxygen concentration (%)	0	5.25	10.5	15.75	21
Ea (kJ/mol)	207.6	200.5	192.3	185.6	181.1

Table 5.
Kinetic parameters obtained for the degradation of cellulose wadding (a in $ln(s^{-1})$.mol/kJ, b in $ln(s^{-1})$, A_2 and A_3 in s^{-1}, Ea_2 and Ea_3 in kJ/mol and Fit in %). f_1, f_2 and f_3 correspond to the contributions under oxidative atmosphere. f_1' and f_3' are the contributions under inert atmosphere.

Kinetic parameters	F_1	F_n	A_n	B_1	D_5
n	1	2.87	0.616	3.24	-
m	-	-	-	1.81	-
a	0.171	0.172	0.183	0.176	0.181
b	1.1878	1.5518	-1.055	1.298	-3.026
f_1	0.580	0.673	0.605	0.685	0.653
f_1'	0.845	0.884	0.853	0.889	0.871
$ln(A_2)$	27.70	27.54	26.56	27.58	26.39
n_2	2.15	2.10	2.40	2.07	2.28
m_2	1.26	1.35	1.14	1.43	1.16
Ea_2	176.0	178.4	172.2	177.7	173.9
f_2	0.330	0.247	0.314	0.236	0.268
$ln(A_3)$	19.83	19.79	17.06	19.84	16.99
Ea_3	189.8	192.8	170.1	193.5	171.0
f_3	0.090	0.080	0.081	0.079	0.079
f_3'	0.155	0.116	0.147	0.111	0.129
Fit	2.32	1.35	1.75	1.31	1.97